Innovative Food Science and Emerging Technologies 20 (2013) 276–280

Contents lists available at ScienceDirect

Innovative Food Science and Emerging Technologies

journal homepage: www.elsevier.com/locate/ifset

The effect of different percent loadings of nanoparticles on the barrier and thermal properties of nylon 6 films

Ahmad R. Allafi [a,*], Melvin A. Pascall [b]

[a] Department of Food Science and Nutrition, College for Women, Kuwait University, P.O. Box 5969, Safat 13060, Kuwait
[b] Department of Food Science and Technology, Ohio State University, 2015 Fyffe Road, Columbus, OH 43210, USA

ARTICLE INFO

Article history:
Received 18 March 2012
Accepted 27 August 2013

Editor Proof Receive Date 12 September 2013

Keywords:
Nylon 6
Nanocomposites
Permeability
Barrier properties
Thermal properties
Melt processing

ABSTRACT

The objective for this study was to investigate the effects of different % loadings on the barrier and thermal properties of nylon 6 nanocomposite materials. Surface modified montmorillonite minerals under the name of Nanomer® I.30T nanoclay were used in this study to produce five different films with varying loading levels of nanoparticles. These films were tested for their permeabilities to oxygen (OTR), carbon dioxide (CO_2TR), and water vapor (WVTR). Thermal properties testing on the samples included differential scanning calorimetry (DSC) and dynamic mechanical analysis (DMA). Results showed that all gas barriers significantly increased with percent loading up to 4% but there were no significant differences ($p > 0.05$) between the 6 and 8% for CO_2TR and OTR at 0 and 50% RH. For the DMA, the storage modulus also significantly increased ($p < 0.05$) with increasing loading except between the 2 and 4% concentrations. For the DSC analyses, enthalpy of fusion decreased slightly from an average of 39 J/g (control) to 32 J/g (8% loading). The melt temperature also decreased from 227 to 222 °C between those loadings.
Industrial relevance: The data collected from this study can be useful to film manufacturers in fabricating nylon nanocomposite materials.

1. Introduction

Different types of repeating monomers produce different nylons. Nylon 6, nylon 6/6, nylon 6/10, nylon 6/12, nylon 11, nylon 12, and nylon 6-6/6 copolymer are the most common. Of these, nylon 6/6 and nylon 6 dominate the packaging market. The numbers refer to the number of methyl units on each side of the amide groups. The number of methyl units influences the property of the various nylons such as moisture absorbance, resistance to thermal deformation and mechanical properties (Zimmerman & Kohan, 2001).

Nylon 6 is one of the most used polymers in the packaging industry (Mohanty & Nayak, 2007). It has a relatively high melting point of 220 °C, which makes it a very good candidate for the manufacturing of retorted food pouches (heat-treated). However, its high permeability to gases in the presence of high moisture causes manufacturers to use special techniques when dealing with this problem (Gorrasi, Incarnato, & Vittoria, 2000). According to Lange and Wyser (2003), in the article entitled "Recent Innovations in Barrier Technologies for plastic packaging — A Review", five different techniques had been developed in order to overcome the problem of low barrier plastics. These methods are thin coatings, new barrier polymers as discrete layers, blends of barrier polymers, organic barrier coatings, and nanocomposite materials. The authors discussed the advantages and disadvantages for each method. Moreover, they stated that incentives such as cost, transparency and convenience are factors influencing the packaging industry in the use of plastics instead of glass or metal for food packaging.

Many studies have supported the use of nanoparticles to enhance the barrier properties of different polymeric materials (Dumont, Reyna-Valencia, Emond, & Bousmina, 2006; Lange & Wyser, 2003). Nanoparticles are very small platelets with at least one dimension measuring less than 100 nm. If deposited and dispersed within a polymer, nanoparticles can create multiple parallel layers which can force diffusing gases to flow through the polymer in a torturous path. This phenomenon results in a reduction in the permeation of the gas through the material (Xu, Zheng, Song, & Shangguan, 2006). Because oxygen and water vapor permeabilities can be reduced when nanocomposite plastics are used, the product's shelf life could be increased without sacrificing quality. Other advantages that nanoparticles impart to polymers include increase mechanical strength, thermal and chemical stabilities and recyclability of certain plastics (Lange & Wyser, 2003).

Many publications have reported the advantages of incorporating nanoparticles into nylon polymers (Dumont et al., 2006; Lange & Wyser, 2003; Xu et al., 2006). However, little has been reported on how the percent loadings of the nanoparticles influence the properties of nylon 6 films. Therefore, this research will provide valuable information about the advantages and disadvantages of the addition of different percentages of nanoparticles to a nylon 6 polymer. Thus, the objectives of this study are to: (1) investigate the influence of nanoparticle percent loadings on the oxygen, carbon dioxide and water vapor transmission

* Corresponding author. Tel.: +965 2498 3161; fax: +965 2251 3929.
E-mail address: ahmadallafi@yahoo.com (A.R. Allafi).

1466-8564/$ – see front matter © 2013 Elsevier Ltd. All rights reserved.
http://dx.doi.org/10.1016/j.ifset.2013.08.009

rates of nylon 6/nanocomposite materials; and (2) determine the impact of the percent loadings on the thermal properties of the nylon 6/nanocomposites.

2. Materials and methods

2.1. Materials and film formulation

The base polymer used in this study was nylon 6 (under the registered name Capron® 8202), supplied by Honeywell Polymers, Inc. (Chicago, IL). The nanoparticles used in this study were Nanomer® I.30T nanoclay, supplied by Nanocor, Inc. (Arlington Heights, IL). This Nanomer® I.30T nanoclay was a surface modified montmorillonite mineral that was used to produce the nanocomposite material. Five different films with varying loading levels of these nanoclay particles were produced with an average thickness of 1.76 ± 0.24 mils. These films had loadings of 0 (as the control), 2, 4, 6, and 8% (wt/wt). A nanoclay/nylon 6 melt compounding process was formulated using a twin-screw extruder at Nanocor's research laboratory (Arlington Heights, IL) to produce the films.

Before processing, nylon pellets and nanomer powder were dried for 8 h in a vacuum oven at 80 °C. Blends were prepared in a Leistritz twin screw extruder (ZSE-27) (L/D = 36:1). Nylon and nanoclay were co-fed into the compounder throat at a rate of 2 kg/h. The extruder was operating at a screw speed of 400 rpm and a temperature profile of 220 °C, 230 °C, and 240 °C from the hopper to the head. The extruded nanocomposite pellets were vacuum re-dried for 12 h for successive film-casting processes. Films were produced using the same extruder used in the mixing step. The extrusion was carried out at a 150 rpm with a temperature profile of 220 °C, 240 °C and 260 °C from the hopper to the head.

2.2. Experimental design

Five films with five different nanoparticle loadings were produced by the melt compounding method. These loadings were 0 (as the control), 2, 4, 6, and 8% (wt/wt). Three replicates from each film were analyzed to determine the following: (1) the effects of nanoparticle loadings on the oxygen, water vapor and carbon dioxide permeabilities of the sample films using a Mocon Oxtran®2/21, a Mocon PEMATRAN-W®3/33 and a Mocon PEMATRAN-C®4/41 permeability testers, respectively; and (2) the effects of nanoparticle loadings on the melt and crystallinity transition temperatures of the film samples using differential scanning calorimetry (DSC) and dynamic mechanical analysis (DMA).

2.3. Permeability testing

2.3.1. Oxygen permeation testing

The oxygen permeabilities of the five different percent nanocomposite films with 0, 2, 4, 6 and 8% loadings were done using the Mocon Oxtran®2/21 permeability tester. These tests were carried out at 23 °C and 1 atm. Three replicates from each film were analyzed to determine the effects of nanoparticle loadings on the permeation of oxygen through nylon 6 films. The tests were repeated at 0, 50 and 80% relative humilities. Prior to performing the test, the films were cut to fit the 50 cm^2 area of the circular test holder of the permeation cell. All samples were conditioned for at least 12 h in the apparatus before commencing the test. During the test, the permeation cell was flushed with oxygen gas on one side and nitrogen carrier gas on the other side. The flow rate of the oxygen gas was 20 cm^3/min while the flow rate of nitrogen was 10 cm^3/min. This nitrogen gas swept any oxygen towards the coulometric sensor for detection. The oxygen permeation of the films ($\frac{cm^3 \ mil}{m^2 \ day}$) was automatically calculated by the software of the attached computer.

2.3.2. Water vapor permeation testing

The water vapor permeabilities of the five different nanocomposite films with 0, 2, 4, 6 and 8% loadings were done using a Mocon PEMATRAN-W®3/33 permeability tester. These tests were carried out at 23 °C, 100% RH and 1 atm. Three replicates from each film were analyzed to determine the effects of nanoparticles on the permeation of water vapor through nylon 6 films. Prior to performing the test, aluminum masks manufactured by Modern Controls Inc. (Minneapolis, MN) were applied to the film samples in order to reduce the test area to 5 cm^2. All samples were conditioned for at least 12 h in the apparatus before commencing the test. During the test, the permeation cell was exposed to a sponge soaked with water on one side and nitrogen carrier gas on the other side. The flow rate of nitrogen was 100 cm^3/min. This nitrogen gas swept any water vapor towards the infrared sensor for detection. The water vapor permeation of the films ($\frac{g \ mil}{m^2 \ day}$) was automatically calculated by the software of the attached computer.

2.3.3. Carbon dioxide permeation testing

The carbon dioxide permeabilities of the five different sets of nanocomposite films were done using a Mocon PEMATRAN-C®4/41 permeability tester. These tests were carried out at 23 °C, 50% RH and 1 atm. Three replicates from each film were analyzed to determine the effects of nanoparticles on the permeation of carbon dioxide through nylon 6 films. Prior to performing the test, the films were cut to fit the 50 cm^2 area of the circular test holder of the permeation cell. All samples were conditioned for at least 12 h in the apparatus before commencing the test. During the test, the permeation cell was flushed with carbon dioxide gas on one side and nitrogen carrier gas on the other side. The flow rate of both carbon dioxide and nitrogen gas was 10 cm^3/min. This nitrogen gas swept any carbon dioxide towards the coulometric sensor for detection. The carbon dioxide permeation of the film ($\frac{cm^3 \ mil}{m^2 \ day}$) was automatically calculated by the software of the attached computer.

2.4. Thermal analysis

2.4.1. Differential scanning calorimetry (DSC)

A TA Instruments Model 2920 Modulated differential scanning calorimeter (DSC) (New Castle, DE), was used to scan the thermal transitions of the 0, 2, 4, 6 and 8% nanoparticle/nylon 6 film samples. The test began by placing 5.1 mg of each sample into individually sealed 30 μl aluminum pans. Each pan was heated under nitrogen purge from 23 °C to 300 °C at a rate of 10 °C/min and then held for 5 min to remove any residual crystals. The sample was then cooled to 23 °C at a rate of 10 °C/min. Thermal parameters such as melting temperature (T_m) and heat of fusion (ΔH_f) were determined from the corresponding transitions in the DSC thermograms. Three replicates from each film were analyzed to determine the effects of nanoparticles on the melting temperature and heat of fusion of nylon 6 films.

2.4.2. Dynamic mechanical analysis (DMA)

The dynamic mechanical analysis was done on all samples using a Rheometrics System Analyzer 3 manufactured by TA Instrument (New castle, DE). The nylon 6 film samples tested had a nanoparticle loading of 0, 2, 4, 6 and 8%. Each sample was cut into small rectangular shapes approximately 35 × 6 mm. All samples had a thickness of 0.05 mm. The temperature range used for this study was 20 to 190 °C at a fixed frequency of 10 Hz and a heating rate of 5 °C/min. Each rectangular shaped film sample was placed in the vertical clamps installed inside the oven of the instrument. Three replicates from each film were tested by the instrument to identify storage and loss moduli and the tan delta of the nanocomposite film samples.

2.5. Morphology testing

2.5.1. Transmission electron microscopy (TEM)

Transmission electron microscopy (TEM) was used in this experiment to examine the dispersion of nanoparticles in the nylon 6 matrix. Film samples for TEM analysis were taken from the middle section of the different films. Ultra-thin sections were cut with a diamond knife at a temperature of −40 °C using a Reichert-Jung Ultracut E microtome. Film samples had a thickness ranged between 70 and 80 nm. Sections were collected on 300 mesh grids and subsequently dried with filter paper. The sections were coated with carbon having a thickness of 20 nm. During the TEM analysis, the film samples were mounted on an electron gun and inserted into the vacuum chamber which was set at 10^{-7} Torr pressure. It was then scanned on a Tecnai F20 STEM instrument manufactured by Fei Company (Hillsboro, OR) at an acceleration voltage of 200 kV. The reflected energy was captured by a detector and transformed into images where the dispersion of nanoparticles in the polymeric matrix was examined.

2.6. Statistical analysis

Data analysis was performed using Statistical Package for Social Sciences (SPSS Inc., Chicago, IL, USA) version 19. Differences in mean values and p-values were tested by analysis of variance (ANOVA) with a 95% confidence interval.

3. Results and discussions

Fig. 1 highlights the barrier improvement of clay nanocomposites against oxygen. Oxygen permeation is reduced from 28.1 to 8.1 $\frac{cm^3 \cdot mil}{m^2 \cdot day}$ for nylon 6 to the 8% loading sample. The statistical analysis shows that there are significant differences ($p < 0.05$) between all nanocomposite films when compared to the pure nylon 6 materials. The statistical analysis also shows that there is a significant difference between oxygen permeation for the 2 and 4% loading. It also shows that the 8% loading has the highest barrier and is significantly different from the 6% loading.

Fig. 2 shows the carbon dioxide permeation for nylon 6, 2, 4, 6, and 8% nylon 6/nanoclay at 23 °C. It can be seen that carbon dioxide permeation for all nanocomposite films shows significant differences ($p < 0.05$) when compared with the pure nylon 6. These differences are confirmed by the statistical analysis using a 95% confidence level. The results are similar to what was obtained for oxygen; however, there is no significant difference ($p > 0.05$) between 6 and 8% loadings.

Fig. 3 highlights the barrier improvement of clay nanocomposites against water vapor. Water vapor permeability is reduced from 593 to 174.7 $\frac{g \cdot mil}{m^2 \cdot day}$. The statistical analysis shows that there are significant differences ($p < 0.05$) between all nanocomposite films when compared to the pure nylon 6 films. It also shows that there are significant differences ($p < 0.05$) within the four loadings of nanoparticles when compared to each other.

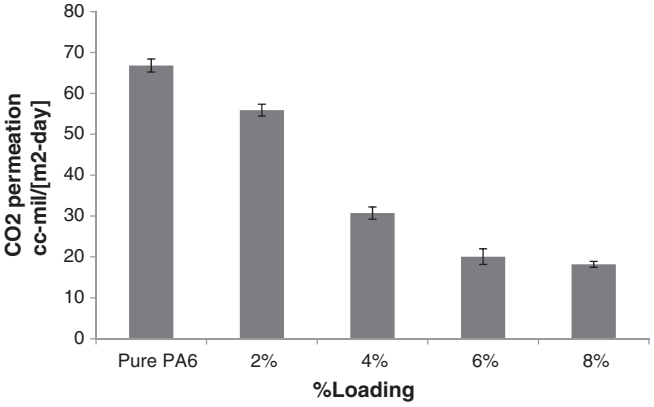

Fig. 2. Carbon dioxide permeation at 50% RH and 23 °C for different nylon 6 nanocomposite loadings.

The reduction in permeations of oxygen, carbon dioxide and water vapor can be explained by the fact that exfoliation of clay nanoparticles and subsequent dispersion through the nylon 6 matrix forces these gases to diffuse through the film in a tortuous path. This can be beneficial to the food industry by the fact that high levels of oxygen present in food packages may facilitate microbial growth, off-flavor and off-odor development, color change, and nutritional losses, thereby causing significant reductions in the shelf life of the product. Therefore, the control of oxygen levels in food packages is important in limiting the rate of these deteriorative and spoilage reactions. Also, the control of moisture in food packages is important if the product is sensitive to water gain or loss. For example, buildup of excess water inside a package could promote bacteria and mold growth in bakery products, resulting in quality loss and shelf life reduction. Finally, high levels of carbon dioxide usually play a beneficial role in retarding microbial growth on meat and poultry surfaces and in delaying the respiration rate of fruits and vegetables. Since carbon dioxide is more permeable than oxygen through many plastic films used for the food packaging, most of the carbon dioxide inside the package usually permeates through the film. For instances nylon 6/nanocomposite films can be used to decrease carbon dioxide permeation and reduce the rate of respiration and suppress microbial growth.

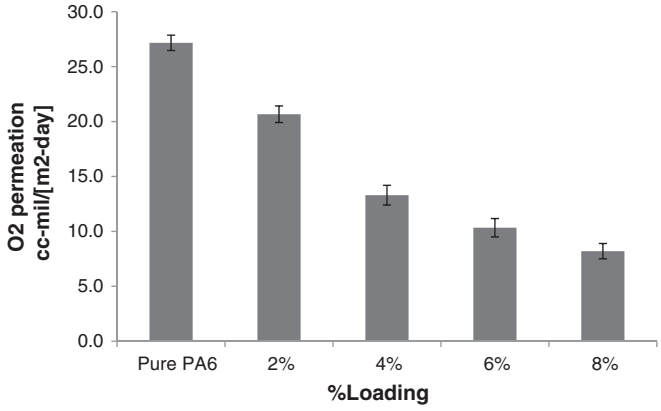

Fig. 1. Oxygen permeation at 50% RH and 23 °C for different nylon 6 nanocomposite loadings.

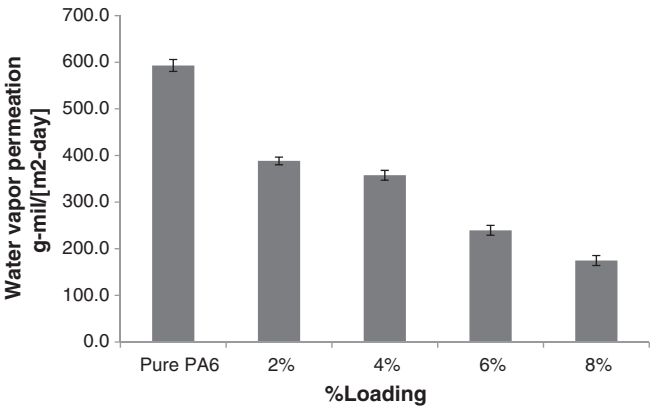

Fig. 3. Water vapor permeation at 50% RH and 23 °C for different nylon 6 nanocomposite loadings.

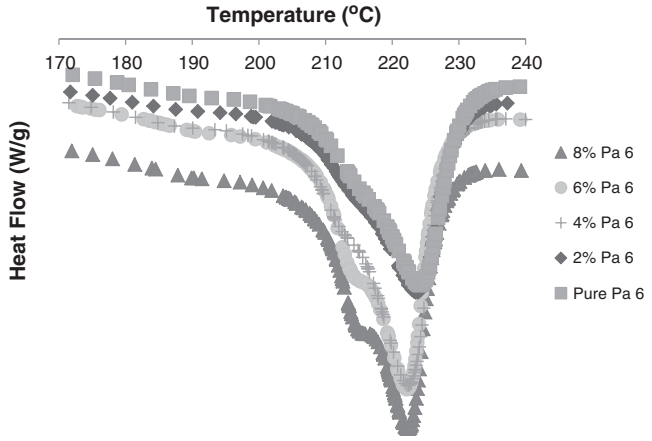

Fig. 4. DSC heating scans for nylon 6, 2%, 4%, 6%, and 8% nylon 6/nanocomposites after heating from room temperature to 300 °C at 10 °C/min.

To elucidate the effect of nanoparticles on the melting behavior of nylon 6/nanocomposites, thermal analysis with DSC was performed. Fig. 4 shows DSC heating scans for nylon 6, 2, 4, 6, and 8% nylon 6/nanocomposites after heating from room temperature to 300 °C at 10 °C/min. The statistical analysis showed that there were significant differences ($p < 0.05$) between all nanocomposite films when compared to the pure nylon 6 films. As seen from the figure, the endothermic peak temperature for pure nylon 6 is located at 224.7 °C. The addition of 2, 4, 6, and 8% nanoparticles led to a decrease in the peak melting temperatures to 224.3 °C, 222.9 °C, 222.4 °C, and 222.1 °C, respectively. This decrease in melting temperatures may be related to the reduction in nylon 6 crystallite size in the presence of nanoparticles. The addition of clay inhibits the formation of large crystals because of limited space and geometric restrictions, which leads to smaller crystallite structures and less ordered crystals. Similar behavior had been investigated for nylon 6/Mg/Al-LDH nanocomposites. Significant decrease in melting temperature of nylon 6 with the addition of 5 wt.% MgAl(H-DS) had been reported (Du, Qu, & Zhang, 2007). Also, it can be seen from Fig. 4 that, as we increase the loading of nanoclays, a second endothermic peak is embedded in the nylon 6/nanocomposite heating scans. Both the height and breadth of these peaks increase with increasing clay content. The presence of a second melting peak may simply reflect imperfections in crystalline structure and its distribution. Similarly, Lincoln, Vaia, Wang, and Hsiao (2001) showed by differential scanning calorimetry and X-ray diffraction experiments on nylon 6/nanocomposites that nanoclay layers disrupt crystallite formation and lead to the formation of less ordered crystals.

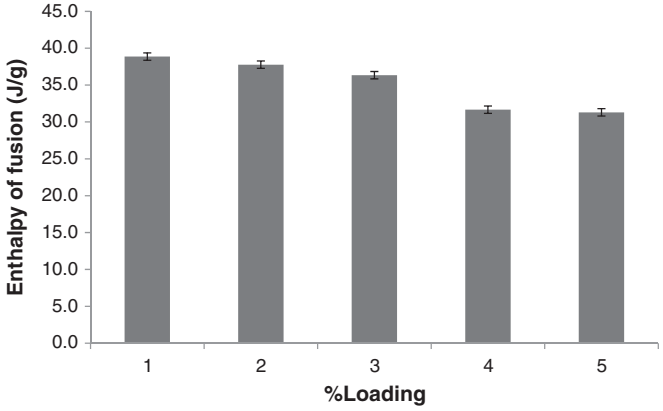

Fig. 5. Enthalpy of fusion for nylon 6, 2, 4, 6, and 8% nylon 6/nanocomposites after heating from room temperature to 300 °C at 10 °C/min.

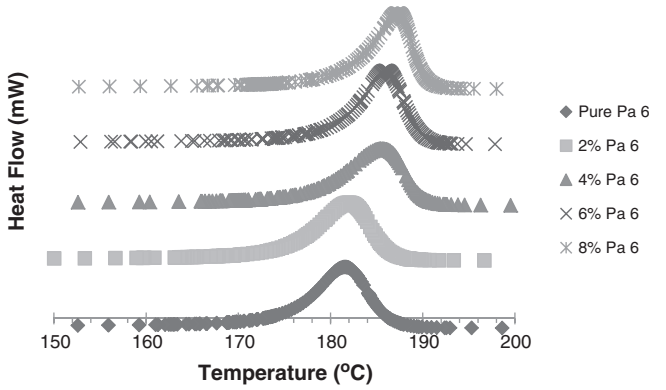

Fig. 6. DSC cooling scans for nylon 6, 2%, 4%, 6%, and 8% nylon 6/nanocomposites after cooling from 300 °C to room temperature at 10 °C/min.

Fig. 5 shows the enthalpy of fusion for nylon 6, 2, 4, 6, and 8% nylon 6/nanocomposites after heating from room temperature to 300 °C at 10 °C/min. The enthalpy of fusion for the five films was calculated by integrating the areas under the DSC heating curves. As seen from the figure, the enthalpies of fusion (1st heat) had values of 38.9, 37.8, 36.3, 31.7, and 31.3 $\frac{J}{g}$ for nylon 6, 2, 4, 6, and 8% nylon 6/nanocomposites, respectively. Statistically speaking, higher loading values were associated with significantly lower heat of fusion. This decrease in the enthalpies of fusions can be explained by the fact that nanoparticles decrease the crystalline structure of nylon 6 and made the peak widths narrower. Since enthalpy of fusion is the heat absorbed per unit weight of a material, the smaller the mass of a substance, the lower is its enthalpy (Baijal, 1982; Höhne et al., 2003).

Fig. 6 shows DSC cooling scans for 0, 2, 4, 6, and 8% nylon 6/nanocomposites after cooling from 300 °C to room temperature at 10 °C/min. The statistical analysis showed that there were significant differences ($p < 0.05$) between all nanocomposite films when compared to the nylon 6 control. As seen from the figure, the exothermic peak temperature for pure nylon 6 is located at 180.9 °C. The addition of 2, 4, 6, and 8% nanoparticles led to an increase in the peak crystallization temperatures to 181.2 °C, 185.1 °C, 185.2 °C, and 186.8 °C, respectively. The above results can be explained by the fact that nanoparticles act as nucleating agents, which have a heterogeneous nucleation effect on the crystallization temperature of nylon 6. The increase of the crystallization temperatures of nylon 6/nanocomposite films is advantageous to the packaging industry since it means that less time is required for the molten resin to solidify after extrusion. This has the potential to significantly accelerate the processing speed of these materials when compared with pure nylon 6. Similar studies by Du et al. (2007) for

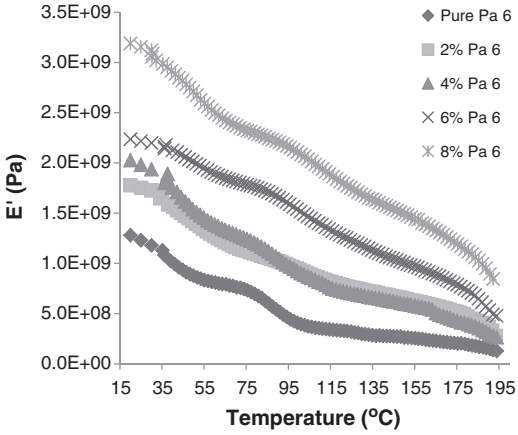

Fig. 7. Variations of storage modulus for nylon 6, 2, 4, 6, and 8% nylon 6/nanocomposites after heating from 20 °C to 190 °C at 5 °C/min.

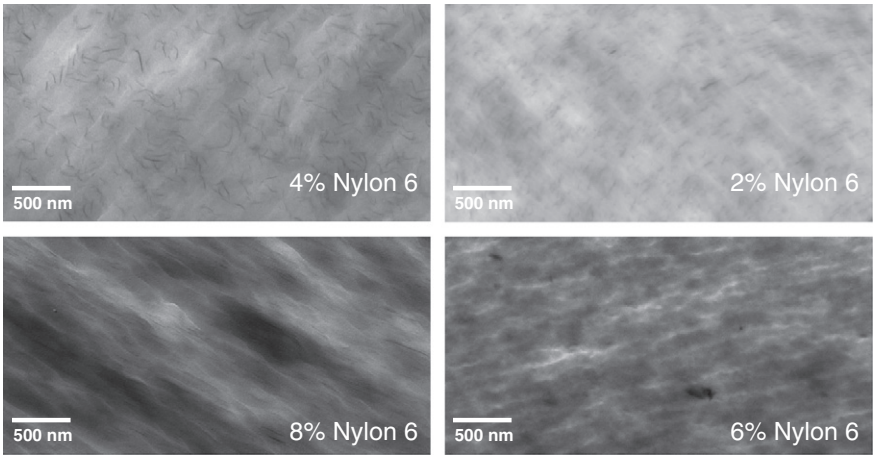

Fig. 8. Transmission electron microscopy of nylon 6 with different nanocomposite loadings.

nylon 6/Mg/Al-LDH nanocomposites showed a significant increase in the crystallization temperature of the nylon 6 after the addition of 5 wt.% MgAl(H-DS) nanoparticles. The increase in the crystallization temperatures seen in Fig. 4 is a result of the nucleating effect of the nanoparticles (Ranade et al., 2003).

The storage modulus obtained from the DMA is shown in Fig. 7 for each of the nylon 6 nanocomposite films. The figure shows data for the storage modulus (E′) after heating from 20 °C to 190 °C at 5 °C/min. The statistical analysis showed that there were significant differences ($p < 0.05$) between all nanocomposite films when compared to the nylon 6 control. It is apparent that the addition of the nanoclay particles increased the storage modulus of all nylon 6 samples in the entire temperature range of the test. This indicates that a reinforcing effect was imparted by the nanoclay particles. Chow, Ishak, Ishiaku, Kocsis, & Apostolov (2004) reported that a high aspect ratio of nanoclay platelets influences a greater degree of stress transfer at the interface between the platelets and the organic polymer. Moreover, limited segmental motion at the organic–inorganic interface, exfoliation of the clay particles and the nanoscale sizes of the particles may be the possible causes for the increase in the storage modulus. Similar behavior had been investigated for polyamide 6/C16 MMT nanocomposites. Data from this polyamide study showed that significant increases in the storage modulus of nylon 6 with the addition of 2.9% MMT clay particles were obtained when compared with pure nylon 6 samples (Liu, Qi, & Zhu, 1999).

The nanometer scale dispersion of nanoparticles in the 2, 4, 6, and 8% loading films is further corroborated with TEM images showed in Fig. 8. It is apparent that, as we increase the loadings, the particles appear more densely distributed. The nanoparticles appear as darker lines. However, for the 8% loading the microgram shows aggregation of the nanoparticles. Thus, it appears that the 6% loading gave the best maximum dispersion without clumping. Thus, it could be concluded that the 6% loading was most desirable.

4. Conclusions

The polymer nanocomposite systems in this study provide improved barrier and thermal properties over pure nylon 6. The barrier improvement for each system was proven with consistent results from oxygen, carbon dioxide, and water vapor permeation tests. The decrease in permeations of these gases can be explained by the fact that exfoliation of nanoparticles and subsequent dispersion through the polymer matrix force these gases to diffuse through the film in a tortuous path.

Thermal testing showed that both melting temperature and enthalpy of fusion decreased with increasing percent loadings. This can be explained by the fact that the addition of nanoparticles inhibits the formation of large crystals because of limited space and geometric restrictions, which leads to smaller and less ordered crystallite structures.

Finally, both crystallization temperature and storage modulus increased with increasing percent loadings. This indicates that nanoparticles act as nucleating and reinforcing agents, respectively.

Conflict of interest declaration

The authors report no conflicts of interest. The authors alone are responsible for the content and writing of the paper.

Role of the funding source

This investigation is part of a doctoral thesis of Ahmad Allafi, who has received a scholarship from the Kuwait University to carry out the study.

Acknowledgments

The authors would like to thank the Kuwait University for the financial support.

References

Baijal, M.D. (1982). Thermal characterization. In A. A. Duswalt (Ed.), *Plastics polymer science and technology* (pp. 201–238). New York: John Wiley & Sons.

Chow, W. S., Ishak, Z. A.M., Ishiaku, U. S., Kocsis, J. K., & Apostolov, A. A. (2004). The effect of organoclay on the mechanical properties and morphology of injection-molded polyamide 6/polypropylene nanocomposites. *Journal of Applied Polymer Science*, *91*, 175–189.

Du, L., Qu, B., & Zhang, M. (2007). Thermal properties and combustion characterization of nylon 6/MgAl-LDH nanocomposites via organic modification and melt intercalation. *Polymer Degradation and Stability*, *92*, 497–502.

Dumont, M., Reyna-Valencia, A., Emond, J., & Bousmina, M. (2006). Barrier properties of polypropylene/organoclay nanocomposites. *Journal of Applied Polymer Science*, *103*, 618–625.

Gorrasi, G., Incarnato, L., & Vittoria, V. (2000). Structural characterization of nylon 6/EvOH system through transport properties. *Journal of Macromolecular Science Part B: Physics*, *39*, 79–92.

Höhne, G. W. H., Hemminger, W. F., & Flammersheim, H. -J. (2003). *Differential scanning calorimetry* (2nd ed.)New Jersey: Springer.

Lange, J., & Wyser, Y. (2003). Recent innovations in barrier technologies for plastic packaging — A review. *Packaging Technology and Science*, *16*, 149–158.

Lincoln, D.M., Vaia, R. A., Wang, Z. -G., & Hsiao, B.S. (2001). Temperature dependence of polymer crystalline morphology in nylon 6/montmorillonite nanocomposites polymer. *Packaging Technology and Science*, *42*, 1621–1631.

Liu, L., Qi, Z., & Zhu, X. (1999). Studies on nylon 6/clay nanocomposites by melt-intercalation process. *Journal of Applied Polymer Science*, *71*, 1133–1138.

Mohanty, S., & Nayak, S. (2007). Effect of clay exfoliation and organic modification on morphological, dynamic mechanical, and thermal behavior of melt compounded polyamide-6 nanocomposites. *Journal of Polymer Composites*, *28*, 153–162.

Xu, B., Zheng, Q., Song, Y., & Shangguan, Y. (2006). Calculating barrier properties of polymer/clay nanocomposites: Effects of clay layers. *Journal of Polymer Science*, *47*, 2904–2910.

Zimmerman, J., & Kohan, M. I. (2001). Nylon-selected topics. *Journal of Polymer Science Part A: Polymer Chemistry*, *39*, 2565-25.